Summary: Effect of core electrical conductivity on core surface flow models

Masaki Matsushima

Department of Earth and Planetary Sciences, Tokyo Institute of Technology

本稿は 2020 年度 Conductivity Anomaly 研究会の論文セッションで発表された Matsushima, M. (2020), Effect of core electrical conductivity on core surface flow models, *Earth, Planets and Space*, **72**:180. https://doi.org/10.1186/s40623-020-01269-0 をまとめたものであり、Matsushima (2020) の本文および図が引用されている。

Abstract

The electrical conductivity of the Earth's core is an important physical parameter that controls the core dynamics and the thermal evolution of the Earth. In this article, the effect of core electrical conductivity on core surface flow models is investigated. Core surface flow is derived from a geomagnetic field model on the presumption that a viscous boundary layer forms at the core–mantle boundary. The core electrical conductivity in the range from $10^5\ \mathrm{S\,m^{-1}}$ to $10^7\ \mathrm{S\,m^{-1}}$ has a limited effect on the tangentially geostrophic core flow. The influence of electrical conductivity on the tangentially magnetostrophic core flow can be clearly recognized; the magnitude of the mean poloidal flow increases with an increase in core electrical conductivity. This arises from the Lorentz force proportional to the electrical conductivity. In other words, the Elsasser number, which represents the ratio of the Lorentz force to the Coriolis force, has an influence on the difference. The result implies that the ratio of toroidal to poloidal flow magnitudes has been changing in accordance with secular changes of rotation rate of the Earth and of core electrical conductivity due to a decrease in core temperature throughout the thermal evolution of the Earth.

Introduction

The magnetic field of the Earth is generated by dynamo action in the outer core. One of basic equations for magnetohydrodynamic dynamo is the induction equation. The core electrical conductivity, σ, is included in the magnetic diffusion term, $\eta\nabla^2\boldsymbol{B}$, of the induction equation, where $\eta=(\mu_0\sigma)^{-1}$ is the magnetic diffusivity, μ_0 the magnetic permeability of vacuum, and $\boldsymbol{B}$ the magnetic field. Another basic equation is the equation of motion. The core electrical conductivity is also included in the Lorentz force term, $\boldsymbol{J}\times\boldsymbol{B}$, of the equation of motion, where $\boldsymbol{J}=\sigma(\boldsymbol{E}+\boldsymbol{V}\times\boldsymbol{B})$ is the electric current density, $\boldsymbol{E}$ the electric field, and $\boldsymbol{V}$ the core flow. Temporal variations of the magnetic field are caused by the motional induction and the magnetic diffusion as given by

$$\dot{\boldsymbol{B}}=\nabla\times(\boldsymbol{V}\times\boldsymbol{B})+\eta\nabla^2\boldsymbol{B},$$

where a dot denotes partial differentiation with respect to time, t. Inversely, core fluid motion can be estimated from a spatial distribution of the geomagnetic field and its temporal variation (e.g., Holme 2015). These relationship is schematically shown in Fig. 0.

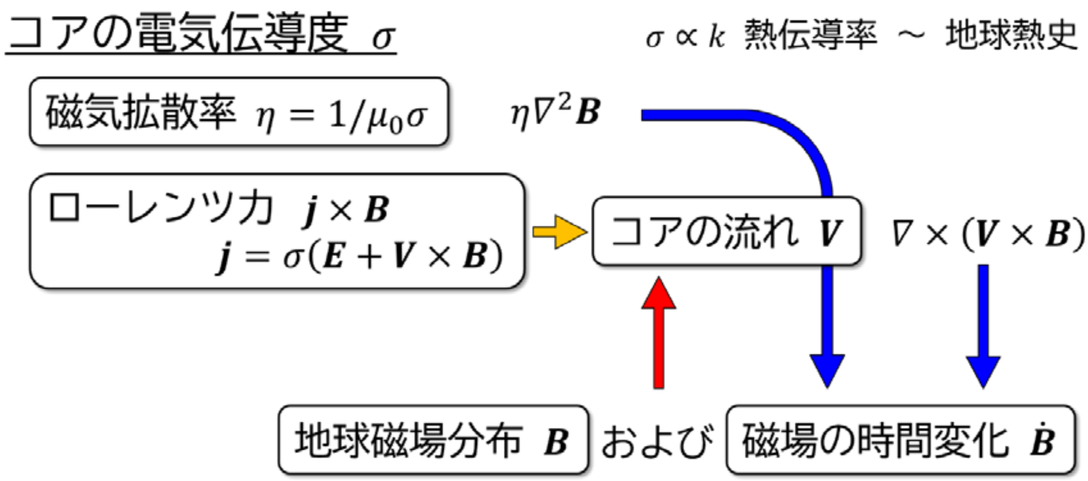

Fig. 0. Schematic view of relationship among effects of motional induction, magnetic diffusion, and Lorentz force on the core flow and the geomagnetic field.

Theory and Method

Most of core surface flow models rely on the frozen-flux approximation (Roberts and Scott 1965), where the magnetic diffusion is neglected due to simple comparison between magnitudes of motional induction and magnetic diffusion terms. However, a viscous boundary layer should be present at the core-mantle boundary (CMB). The magnetic diffusion inside such a boundary layer is found to play an important role in temporal variations of the geomagnetic field (Takahashi et al. 2001). Therefore, an approach to estimate fluid motion near the CMB has been devised by Matsushima (2015); the magnetic diffusion is explicitly incorporated within the viscous boundary layer at the CMB, while the magnetic diffusion is neglected below the boundary layer. Matsushima (2015) assumed that fluid motion below the boundary layer is tangentially geostrophic, which means that the Lorentz force was not taken into account. To examine the effect of core electrical conductivity on a core flow model, fluid motion is assumed to be tangentially magnetostrophic below the boundary layer.

To estimate core flow near the CMB, the radial component of induction equation is solved with the magnetostrophic constraint. The equations to be solved are given as follows;

$$\dot{\boldsymbol{B}}_{r1} = -(\boldsymbol{V}_1 \cdot \nabla)B_{r1} + (\boldsymbol{B}_1 \cdot \nabla)V_{r1} + \frac{\eta}{r_1}\nabla^2(r_1 B_{r1}), \tag{1a}$$

$$\dot{\boldsymbol{B}}_{r2} = -(\boldsymbol{V}_2 \cdot \nabla)B_{r2} + (\boldsymbol{B}_2 \cdot \nabla)V_{r2}, \tag{1b}$$

$$\nabla_H \cdot \left(2\Omega\cos\theta\,\overline{\boldsymbol{V}}_H + \frac{\sigma B_{r2}^2}{\rho}\overline{\boldsymbol{V}}_H \times \hat{\boldsymbol{r}}\right) = 0, \tag{1c}$$

where subscripts r and H denote the radial and horizontal components, respectively, subscripts 1 and 2 indicate depths from the CMB (assumed to be a spherical surface of radius $r = r_0 = 3480$ km) as $r = r_1 = r_0 - \xi_1$ (inside the boundary layer) and $r = r_2 = r_0 - \xi_2$ (below the boundary layer), respectively. $\Omega = 7.29 \times 10^{-5}\ \mathrm{rad\ s^{-1}}$ denotes the angular velocity of the mantle, $\rho = 1.1 \times 10^4\ \mathrm{kg\ m^{-3}}$ the mass density of core fluid, $\hat{\boldsymbol{r}}$ the radial unit vector, and θ the colatitude in the spherical coordinates (r, θ, ϕ). The horizontal flow, $\boldsymbol{V}_H$, near the core surface can be expressed as

$$\boldsymbol{V}_H = \overline{\boldsymbol{V}}_H \left\{1 - \exp\left(-\frac{\xi}{\delta_{EH}^{+}}\right)\cos\left(\frac{\xi}{\delta_{EH}^{-}}\right)\right\} + (\operatorname{sgn}\cos\theta)\hat{\boldsymbol{r}} \times \overline{\boldsymbol{V}}_H \exp\left(-\frac{\xi}{\delta_{EH}^{+}}\right)\sin\left(\frac{\xi}{\delta_{EH}^{-}}\right), \quad (2)$$

where $\overline{\boldsymbol{V}}_H$ is the tangentially magnetostrophic flow far below the Ekman-Hartmann boundary layer, sgn is the signum function,

$$\delta_{EH}^{\pm} = \frac{\delta_E}{\{(1 + \Lambda^2/4)^{1/2} \pm \Lambda/2\}^{1/2}} \quad (3)$$

(double sign correspondence), $\delta_E = (\nu_{\mathrm{edd}}/\Omega|\cos\theta|)^{1/2}$, ν_{edd} is the eddy kinematic viscosity assumed to be $5\ \mathrm{m}^2\ \mathrm{s}^{-1}$ in this study, and

$$\Lambda = \frac{\sigma B_r^2}{\rho\Omega|\cos\theta|} \quad (4)$$

is the Elsasser number. The horizontal magnetostrophic flow can be expressed in terms of poloidal and toroidal constituents, and their scalar functions, which are expanded into spherical harmonics, are calculated. The electrical conductivity of outer core, as a parameter, is investigated in the range from $\sigma = 10^5\ \mathrm{S\ m^{-1}}$ to $\sigma = 10^7\ \mathrm{S\ m^{-1}}$.

To obtain a core surface flow model, a geomagnetic field model COV-OBS.x1 (Gillet et al. 2015) is adopted. The magnetic field at the CMB is derived through downward continuation of a geomagnetic potential field by assuming the mantle to be electrically insulating. The truncation level of spherical harmonic coefficients is set at degree 14.

Results

First, the effect of core electrical conductivity on tangentially geostrophic core flow near the CMB is investigated. Correlation coefficients of $\nabla_H \cdot \boldsymbol{V}_H$ and $\hat{\boldsymbol{r}} \cdot \nabla \times \boldsymbol{V}_H$, which correspond to those of the poloidal and toroidal components, respectively, are computed between the one for $\sigma = 10^6\ \mathrm{S\ m^{-1}}$ and that for other σ in the range between $10^5\ \mathrm{S\ m^{-1}}$ and $10^7\ \mathrm{S\ m^{-1}}$. The correlation coefficients are found to be at least 0.98. The mean velocity over spherical surfaces at $r = r_1$ and at $r = r_2$ for $\sigma = 10^6\ \mathrm{S\ m^{-1}}$ is also found to be nearly the same as those for other σ in the range between $10^5\ \mathrm{S\ m^{-1}}$ and $10^7\ \mathrm{S\ m^{-1}}$. The result implies that core electrical conductivity has a limited effect on core flow models through the magnetic diffusion term under the tangentially geostrophic constraint.

Secondly, the effect of core electrical conductivity on tangentially magnetostrophic flow below the boundary layer at the CMB is investigated. Figures 1a-c show fluid motions near the CMB at $r = r_1$ and at $r = r_2$ for $\sigma = 10^5\ \mathrm{S\ m^{-1}}$, $\sigma = 10^6\ \mathrm{S\ m^{-1}}$, and $\sigma = 10^7\ \mathrm{S\ m^{-1}}$, respectively, at the epoch of 2010. Core flows for $\sigma = 10^5\ \mathrm{S\ m^{-1}}$ are similar to those for $\sigma = 10^6\ \mathrm{S\ m^{-1}}$, whereas those for $\sigma = 10^7\ \mathrm{S\ m^{-1}}$ are obviously different from those for $\sigma = 10^6\ \mathrm{S\ m^{-1}}$. The horizontal divergence for $\sigma = 10^7\ \mathrm{S\ m^{-1}}$ appears larger than that for $\sigma = 10^6\ \mathrm{S\ m^{-1}}$. Figure 2 shows the dependence of poloidal and toroidal mean-flow magnitudes on the core electrical conductivity. The mean velocity for the toroidal component does not vary irrespective of core electrical conductivity, whereas that for the poloidal component increases with increasing core electrical conductivity, as found from larger horizontal divergence for higher electrical conductivity.

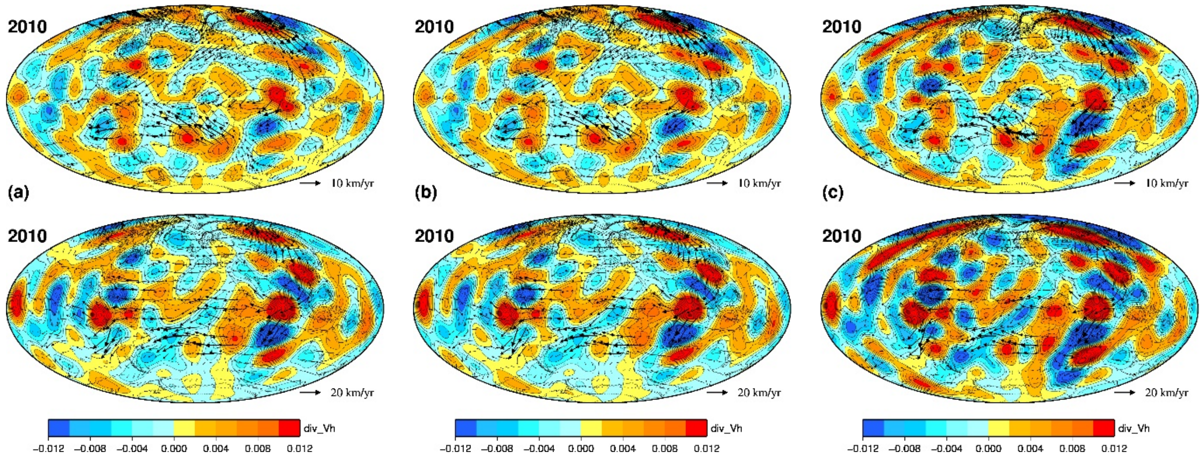

Fig. 1. Fluid motion near the core-mantle boundary under the tangentially magnetostrophic constraint. Upper and lower figures show fluid motions at $r = r_1$ and at $r = r_2$, respectively, for (a) $\sigma = 10^5\ \mathrm{S\,m^{-1}}$, (b) $\sigma = 10^6\ \mathrm{S\,m^{-1}}$, and (c) $\sigma = 10^7\ \mathrm{S\,m^{-1}}$ at the epoch of 2010. Arrows show the horizontal flows, and color contours denote upwellings and downwellings given by $\nabla_H \cdot \boldsymbol{V}$.

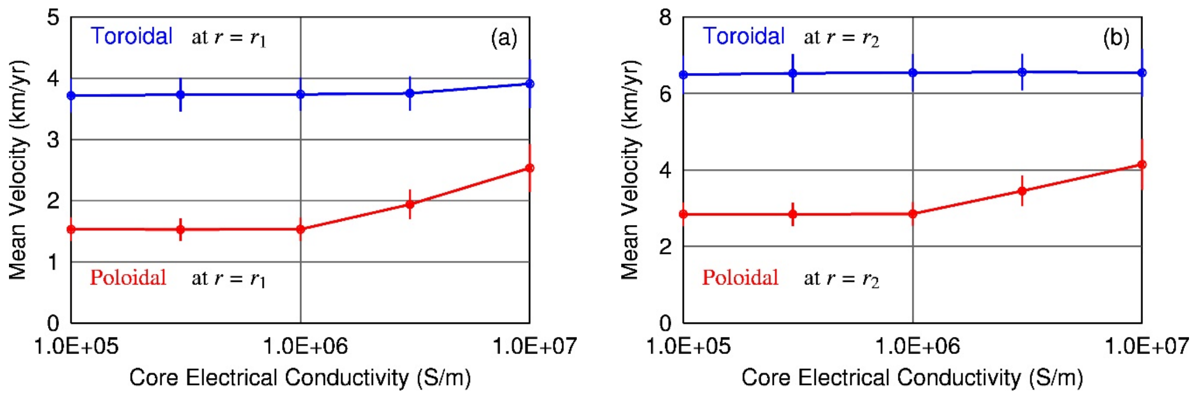

Fig. 2. Mean toroidal and poloidal velocity with respect to the core electrical conductivity. Circles and error bars represent means and $\pm$standard deviations, respectively, obtained for COV-OBS.x1 (Gillet et al. 2015) ranging from 1880 to 2015, at (a) $r = r_1$ and (b) $r = r_2$.

Discussion

To determine the cause of electrical conductivity dependence as above, mean flow velocity is examined under the tangentially geostrophic and tangentially magnetostrophic constraints. The ratio of the mean toroidal flow to the mean poloidal flow magnitudes at $r = r_2$ under the tangentially geostrophic constraint is computed for spherical harmonic order $m = 1$ to $m = 6$ by minimizing the following function, Ψ_g:

$$\Psi_g = [\nabla_H \cdot (\cos\theta\, \overline{\boldsymbol{V}}_H)]^2 + \alpha_g \int \left\{ (\overline{V}_{\theta 2})^2 + \left(\overline{V}_{\phi 2}\right)^2 \right\} dS, \tag{5}$$

where α_g is a controlling parameter. Figure 3 shows the velocity ratio, which is found to be approximately 2 for smaller α_g.

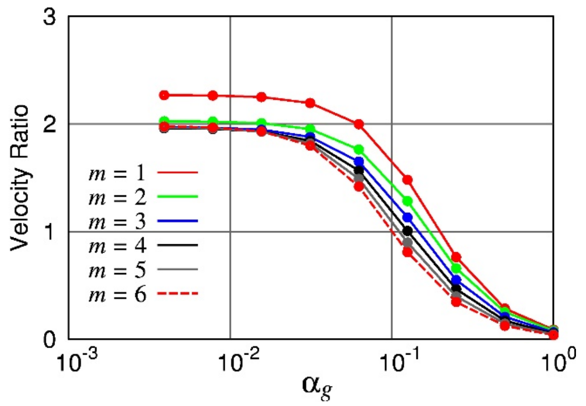

Fig. 3. Control parameter, α_g, dependence of toroidal and poloidal mean flow ratios. Circles represent the ratio of the mean toroidal flow to the mean poloidal flow magnitudes at $r = r_2$ under the tangentially geostrophic constraint, for spherical harmonic order $m = 1$ to $m = 6$.

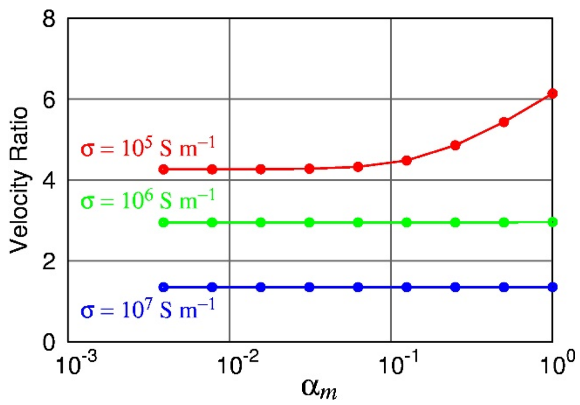

Fig. 4. Control parameter, α_m, dependence of toroidal to poloidal mean flow ratios. Circles represent the ratio of the mean toroidal to the mean poloidal flow magnitudes at $r = r_2$ under the tangentially magnetostrophic constraint, for $\sigma = 10^5\ \mathrm{S\,m^{-1}}$, $\sigma = 10^6\ \mathrm{S\,m^{-1}}$, and $\sigma = 10^7\ \mathrm{S\,m^{-1}}$ at the epoch of 2010.

Next, the ratio of the mean toroidal flow to the mean poloidal flow magnitudes under the tangentially magnetostrophic constraint is computed by minimizing the function, Ψ_m;

$$\Psi_m = [\nabla_H \cdot (\cos\theta\, \overline{\boldsymbol{V}}_H + \rho^{-1}\sigma B_{r2}^2 \overline{\boldsymbol{V}}_H \times \hat{\boldsymbol{r}})]^2 + \alpha_m \int \left\{(\bar{V}_{\theta 2})^2 + \left(\bar{V}_{\phi 2}\right)^2\right\} dS, \tag{6}$$

where α_m is a controlling parameter. Figure 4 shows the velocity ratio for $\sigma = 10^5\ \mathrm{S\,m^{-1}}$, $10^6\ \mathrm{S\,m^{-1}}$, and $10^7\ \mathrm{S\,m^{-1}}$. The velocity ratio clearly decreases with increasing σ, which means that the magnitude of mean poloidal flow increases relatively to that of mean toroidal flow. It is likely that this result arises from the effect of the Lorentz force proportional to σ.

Asari and Lesur (2011) found that the tangentially geostrophic constraint mainly influences the poloidal flow, and pointed out that the tangentially magnetostrophic constraint rather mitigates the poloidal flow. This may be related with the present result that the magnitude of mean poloidal flow increases with increasing core electrical conductivity.

It should be pointed out that the tangentially magnetostrophic constraint does not depend on core electrical conductivity alone, as found in Eq. (1c). The importance of the Lorentz force relative to the Coriolis force can be measured by the Elsasser number, Λ, as given by Eq. (4). The rotation rate of the Earth has been decreasing due to tidal friction with the Moon. The rotation period is currently approximately 24 hours, but it could have been as little as 4–6 hours immediately after the Moon formed (e.g., Goldreich 1966). This means that Ω was about six to four times larger than the present value. On the other hand, the core temperature has been decreasing since the formation of the core. This implies that the core electrical conductivity in the past could have been lower than the present value. In short, the rotation rate of the Earth decreases, and the core electrical conductivity increases with time. These indicate that the denominator of $\Lambda = \sigma B_r^2/\rho\Omega|\cos\theta|$ has been decreasing, and that the numerator of Λ has been increasing, throughout the history of the Earth. That is, the Elsasser number, Λ, could have been smaller in the past than at present, and Λ will be increasing. This implies that core flow in the past could have been more geostrophic than the present flow state, and that the style of magnetic field generation by poloidal and toroidal motions in the core has been changing.

Conclusions

In this article, the effect of core electrical conductivity on core surface flow models was investigated. It was found that core electrical conductivity in the range between $10^5\ \mathrm{S\,m^{-1}}$ and $10^7\ \mathrm{S\,m^{-1}}$ has a limited effect on core flow models under the tangentially geostrophic constraint. In contrast, the mean poloidal flow increases with an increase of core electrical conductivity under the tangentially magnetostrophic constraint. This results from the Lorentz force proportional to core electrical conductivity which is likely to be stronger than the Coriolis force. The Elsasser number given by the ratio of the Lorentz to Coriolis forces has been increasing throughout the evolution of the Earth, because the rotation rate of the Earth has been decreasing and the core electrical conductivity has been increasing due to the decrease in core temperature. These results imply that the ratio of the magnitude of mean toroidal flow to that of mean poloidal flow has been changing with secular change of the Elsasser number; that is, the style of magnetic field generation by poloidal and toroidal flows in the core has been changing throughout the evolution of the Earth.

References

Asari, S., Lesur, V. (2011) Radial vorticity constraint in core flow modeling. *J. Geophys. Res.*, **116**:B11101.

Gillet, N., Barrois, O., Finlay, C. C. (2015) Stochastic forecasting of the geomagnetic field from the COV-OBS.x1 geomagnetic field model, and candidate models for IGRF-12. *Earth Planets Space*, **67**:71.

Goldreich, P. (1966) History of the lunar orbit. *Rev. Geophys.*, **4**:411-439.

Holme, R. (2015) Large-scale flow in the core. In *Treatise on Geophysics* edited by Olson, P., 2nd ed., vol. 8, Elsevier, Amsterdam.

Matsushima, M. (2015) Core surface flow modelling with geomagnetic diffusion in a boundary layer. *Geophys. J. Int.*, **202**:1495-1504.

Matsushima, M. (2020) Effect of core electrical conductivity on core surface flow models. *Earth Planets Space*, **72**:180.

Roberts, P. H., Scott, S. (1965) On analysis of the secular variations, 1: A hydromagnetic constraint: theory, *J. Geomag. Geoelectr.*, **17**, 137-151.

Takahashi, F., Katayama, J. S., Matsushima, M., Honkura, Y. (2001) Effects of boundary layer on magnetic field behavior in an MHD dynamo model. *Phys. Earth Planet. Int.*, **128**, 149-161.